Electric-field poling effect on thermal stability of monoclinic phase in Pb(Mg1/3Nb2/3)0.74Ti0.26O3 single crystal

Authors: R. R. Chien, V. Hugo Schmidt, and C.-S. Tu

R.R. Chien, V.H. Schmidt, and C.-S. Tu, "Electric-field poling effect on thermal stability of monoclinic phase in Pb(Mg1/3Nb2/3)0.74Ti0.26O3 single crystal," J. Crystal Growth 287, 454-457 (2006). doi: 10.1016/j.jcrysgro.2005.11.065.

Electric-field poling effect on thermal stability of monoclinic phase in $Pb(Mg_{1/3}Nb_{2/3})_{0.74}Ti_{0.26}O_3$ single crystal

R.R. Chien[a,*], V. Hugo Schmidt[a], Chi-Shun Tu[b]

[a]*Department of Physics, Montana State University, #264 EPS Building, Bozeman, MT 59717, USA*
[b]*Graduate Institute of Applied Science and Engineering, Fu Jen University, Taipei 242, Taiwan*

Available online 4 January 2006

Abstract

Phases and domains in a (1 1 0)-cut $Pb(Mg_{1/3}Nb_{2/3})_{0.74}Ti_{0.26}O_3$ (PMNT26%) single crystal have been investigated as functions of temperature and direct current (DC) electric (E) field by dielectric permittivity, polarizing microscopy, and electric polarization. The unpoled sample has a dominant rhombohedral (R) phase coexisting with monoclinic (M) phase domains, i.e. R/M at room temperature (RT). With 45 kV/cm DC poling applied along [1 1 0] at RT, a single domain of R phase with polar orientation perpendicular to the poling field, i.e. R, was obtained. No microcracking was observed under such high DC field poling. After the poling was removed, the poled sample has R/M microdomains, where the M distortion is close to the R phase. The zero-field-heating domain patterns in the unpoled and poled samples exhibit continuous polarization rotation via an intrinsic M phase in the regions of 355–373 and 365–378 K, respectively. Orthohombic (O) and tetragonal (T) phases were not observed in the temperature-dependent study. The whole crystal becomes cubic (C) phase near 393 and 399 K in the unpoled and poled sample, respectively. In brief, an R/M→M→C transition sequence takes place upon heating for both unpoled and poled samples.

PACS: 77.84.Dy; 77.80.Bh; 77.22.Ej; 77.22.Ch

Keywords: A1. Domain; A1. Electric-field poling; A1. Phase transitions; B1. PMN-PT crystal

1. Introduction

High-strain ferroelectric $Pb(Mg_{1/3}Nb_{2/3})_{1-x}Ti_xO_3$ (PMNTx) and $Pb(Zn_{1/3}Nb_{2/3})_{1-x}Ti_xO_3$ (PZNTx) single crystals have drawn much attention because of their superior electromechanical properties compared to lead zirconate titanate (PZT) ceramics, and therefore have great potential for designing high-performance actuators and sensors. Physical properties of PMNT and PZNT crystals strongly depend on titanium (Ti) content, temperature, E-field poling strength, crystallographic orientation, and history. The crystal structures can occur in the C, T, O, R, M, and triclinic (Tri) phases. All the phases except Tri phase have been observed in PMNT crystals. The ultrahigh piezoelectric response has been theoretically attributed to polarization rotation induced by an external E-field between T and R phases through intermediate M or O symmetries [1]. To understand the E-field effect on phase transition, here we study thermally induced phase transitions in both unpoled and poled (1 1 0)-cut PMNT26% samples.

2. Experimental procedure

The PMNT26% single crystal was grown using a modified Bridgman method and was cut perpendicular to the ⟨1 1 0⟩ direction. Gold electrodes deposited by DC sputtering were used for dielectric measurement. A Wayne–Kerr Precision Analyzer PMA3260A was used to obtain capacitance and resistance. A Janis CCS-450 cold-head was used with a Lakeshore 340 temperature controller and the ramping rate was 1.5 K/min. Two processes were used in the dielectric measurements. The first is called

"zero-field-heating" (ZFH), in which the data were taken upon heating without any *E*-field poling. The second process is called FR-ZFH, in which the sample was poled at RT before ZFH was performed. The domain observation was studied by using a Nikon E600POL polarizing microscope mounted with a Linkam THMS600 heating/cooling stage. To minimize the superposition of domains, the sample was polished to the thickness of 45 μm. Transparent conductive films of indium tin oxide (ITO) were deposited on the sample by sputtering for domain observation. The experimental configuration for domain study can be found in Ref. [2]. The [0 0 1] orientation of the sample edge was determined by X-ray diffraction and aligned with one of the crossed polarizer/analyzer (P/A): 0° axes so that the extinction angles shown in all domain pictures are measured from [0 0 1]. Hysteresis loop of polarization vs. *E*-field was taken by using a Sawyer–-Tower circuit at 46 Hz.

3. Results and discussion

A broad dielectric maximum $T_m = 390$ K and a weak shoulder (as indicated by an arrow) near 370 K, as shown in Fig. 1, were evidenced in the ε'(ZFH). However, the FR-ZFH dielectric data (with prior polings at 0.75 and 4 kV/cm) exhibit an extra sharp peak associated with one weak shoulder at its right side. Correspondingly, ε''(FR-ZFH) exhibits, respectively, two frequency-independent peaks (superimposed on a broad maximum background) near 365 and 373 K. Similar field-induced dielectric phenomena were found in other oriented poled PMNT crystals [3].

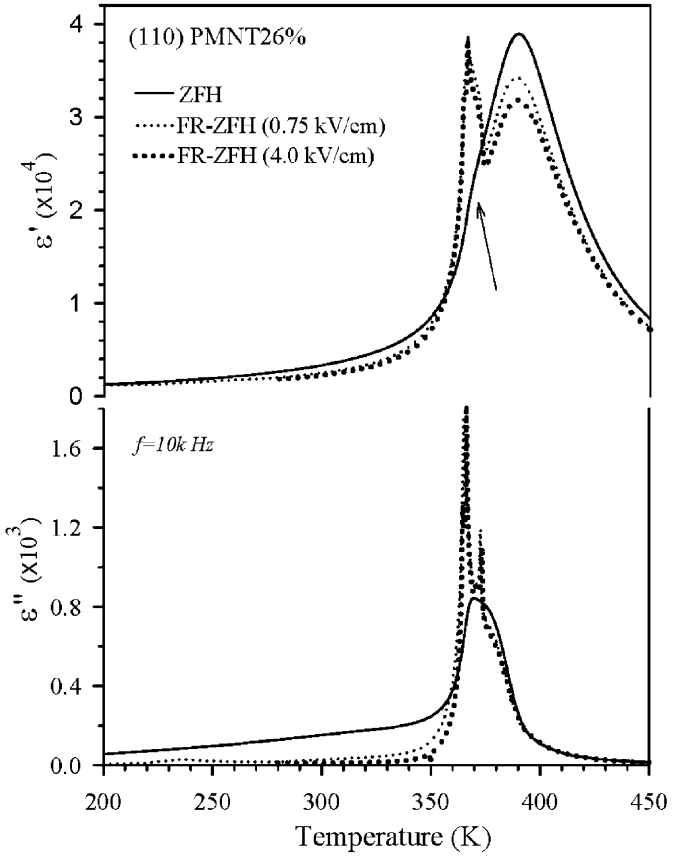

Fig. 1. ZFH and FR-ZFH (0.75 and 4 kV/cm) dielectric permittivities obtained at $f = 10$ kHz.

By using relations of crystallographic symmetry and optical extinction, polarizing microscopy reveals orientations of the polarizations and their corresponding phases. For interpreting domain observation among various phases by means of polarizing microscopy, a review of principles of optical extinction for (1 1 0)-cut crystal can be found in Ref. [4]. R domains represented by triangles in Fig. 2 have extinction at 0° (= 90°), 35°, and 55°, which were shown by the solid crosses in the triangles. The extinction angles are measured with regards to [0 0 1]. T domains represented by squares with solid crosses have extinction at 0° (or 90°). For the O domains represented by open circles with no cross, the optical biaxiality of the O structure means that the extinction orientations are not known unless all three indices of refraction along the axes of the double-size ($Z = 2$) O cell are known, so we cannot identify such domains by their extinction angles because we do not know these indices. Any extinctions at angles other than 0° (or 90°), 35°, and 55° must be from these open-circle O domains, M domains, or Tri domains. Our large observed variation in extinction angle with temperature indicates M domains whose polarization P can vary with temperature through a large angle, whereas the direction of P is nearly fixed for a given open-circle O domain as temperature varies.

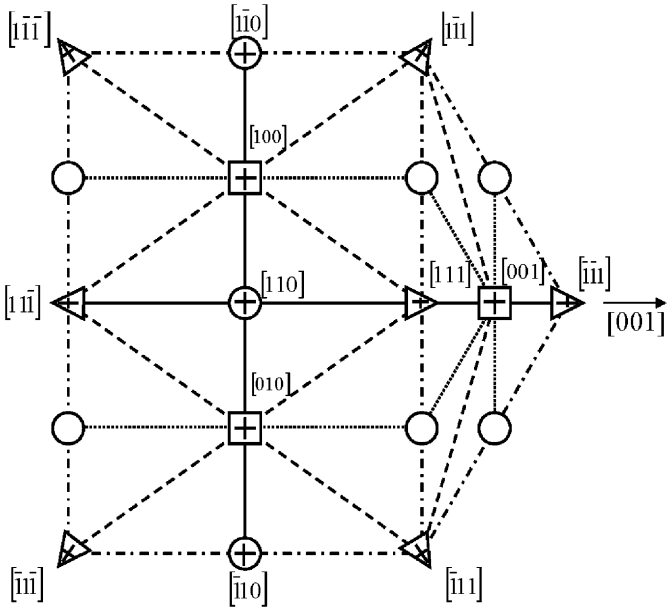

Fig. 2. Projection of the optical extinction orientations on the (1 1 0) plane for various polarizations of domains. For instance, the R domains (triangles) measured from [0 0 1] give extinction at 0° (or 90°), 35°, and 55°. The T (squares) and O (circles with solid cross) domains also give extinction at 0° (or 90°). Dashed, dash-dotted, and dotted lines represent M_A, M_B, and M_C domains, respectively.

The obtained extinction angles in various domains were written with numbers and indicated by arrows in the domain micrographs in Fig. 3.

At RT, a larger fraction of the unpoled sample exhibits extinction at P/A: 0° and 85–90°, and a small fraction exhibits extinctions at P/A: 45–60° and 35–55°. This indicates that the unpoled sample has a dominant R phase with polar orientation [1 1 1], [1 1 $\bar{1}$], and/or [$\bar{1}$ $\bar{1}$ 1] that coexists with M phase domains, i.e. R/M. R/M represents more R than M phase domains [Fig. 3(a)]. As the field increases to ~3.5 kV/cm, part of the domain matrix exhibits obvious change in birefringence and has extinction angles at 55–60 ° [see Fig. 3(b)]. Note that the coercive field is E_c ~3 kV/cm as shown in Fig. 3(h). The extinction at 55–60° indicates appearance of another oriented R phase domain (denoted by R), possible mixed with M domain. The R phase domains have extinction at 55°. The possible orientations are along [1 $\bar{1}$ 1], [$\bar{1}$ 1 $\bar{1}$], [1 $\bar{1}$ $\bar{1}$], and/or [$\bar{1}$ 1 1]. The R phase domain expands with poling strength as seen in Figs. 3(c) and (d), in which the weaving domain walls exhibit no optical extinction at all P/A angles. The whole domain matrix was dramatically affected by the poling at 4.6 kV/cm [Fig. 3(d)]. The weaving domain walls gradually disappear as *E*-field strength increases, as seen in Fig. 3(e). Some domain walls persist to E ~26 kV/cm but disappear after poling at this strength for more than 3 h. The domain matrix almost reaches a R phase monodomain at $E = 45$ kV/cm [Fig. 3(f)].

An O phase polarized along [1 1 0] might be expected when such high-field poling was applied along [1 1 0]. There will be extinction at P/A: 0° if such an O phase domain exists. However, as shown in Fig. 3(f), no extinction at

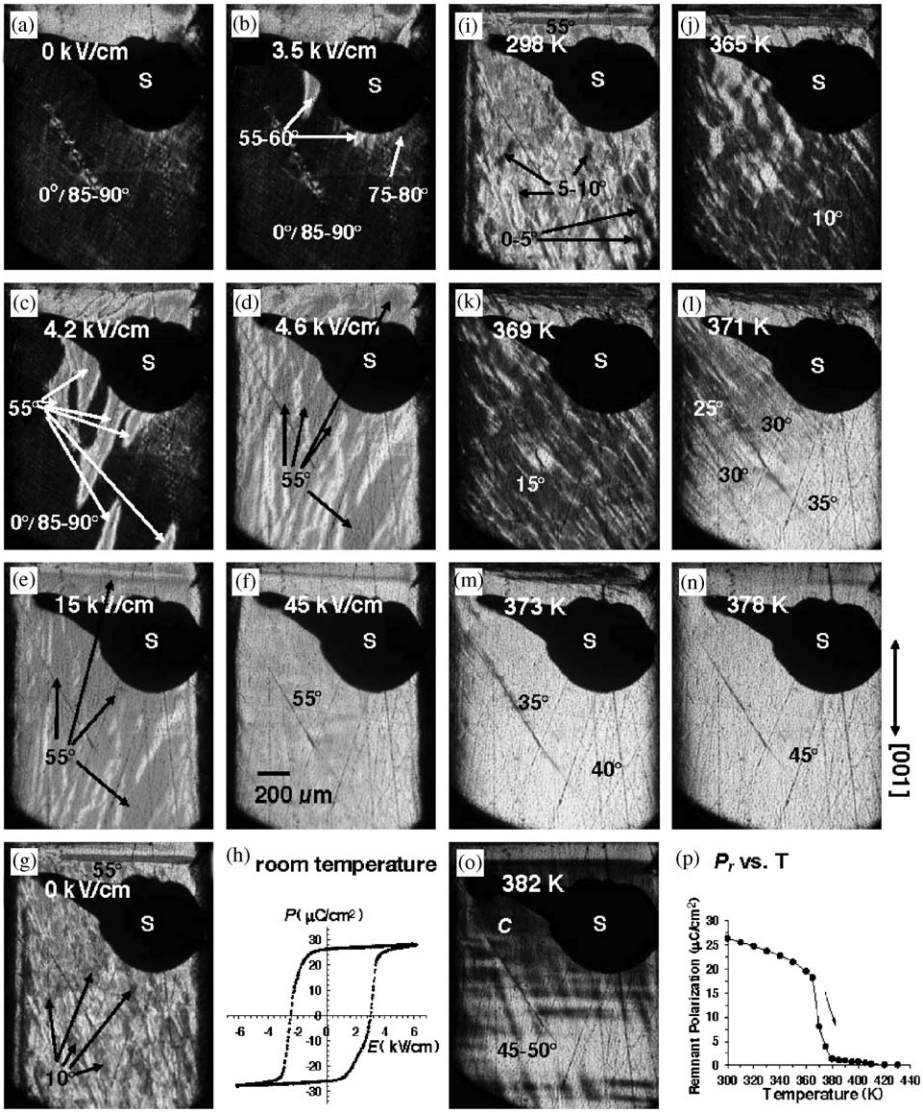

Fig. 3. *E*-field-dependent domains observed at RT for: (a) 0 kV/cm, (b) 3.5 kV/cm, (c) 4.2 kV/cm, (d) 4.6 kV/cm, (e) 15 kV/cm, (f) 45 kV/cm, and (g) right after the *E*-field was removed. (h) Hysteresis loop of polarization vs. *E*-field obtained at RT. (i)–(o) ZFH domain structures observed 27 days later after poling. All domain micrographs were taken at P/A: 0°. The angles written in the domain matrix indicate the extinction angles in that area. "S" represents silver paste. "C" indicates cubic phase. (p) Remnant polarization (μC/cm^2) vs. temperature upon heating.

P/A: 0° was observed. Instead, the extinction appears at P/A: 55°, which corresponds to the R phase. Under poling at 45 kV/cm, microcracking was not found. After the field was removed [Fig. 3(g)], the crystal does not re-establish the R/M phase macrodomains, but instead breaks up into M/R microdomains indicated by the extinction angles 10 and 55°. About more than one-half of the domain matrix does not have optical extinction, perhaps due to the local stress caused by various polar microdomains. Twenty-seven days after the field was removed, ZFH domain observation was performed. As shown in Fig. 3(i), the crystal birefringence at RT has been changed a little, and the M domains with extinction at 10° [Fig. 3(g)] change their extinction angle to 0–5° and 5–10°. This indicates that the polarizations have relaxed to different M symmetries that are close to R symmetry. As temperature increases to 365 K [Fig. 3(j)], the domain matrix exhibits change in extinction angle and birefringence. Correspondingly, the remnant polarization also exhibits apparent drop [Fig. 3(p)] near 365 K. Most domains exhibit extinction at 10° and few domains at 55°, which correlates to M(R) phase. M(R) represents much more M than R phase domains.

With increasing temperature, the extinction angle changes continuously from 10° to 45° [Fig. 3(j)–(n)], indicating that the crystal exhibits continuous polarization rotation via M phase from 365 to 378 K. This polarization rotation through the M phase ends above 378 K. In addition, the poled sample exhibits domain boundaries [Fig. 3(i)–(l)] between the R and M phase domains and some of these boundaries persist to ~373 K [Fig. 3(m)]. As temperature increases to 382 K, C phase starts to appear [Fig. 3(o)] and no T phase was observed. The whole crystal becomes cubic near 399 K. In brief, the temperature-dependent transition sequences in the prior poled sample are R/M/R → M(R) → M → C for the prior poling of 3.5–4.6 kV/cm and R → M(R) → M → C for the prior poling $E \geqslant 4.6$ kV/cm. We also observed temperature-dependent phase transition and polarization rotation via the M phase near 355–373 K in the unpoled sample, the same range in which sharp dielectric permittivity anomalies were observed to be more pronounced in the poled sample.

4. Conclusions

The phase transition sequence, R/M → M → C, takes place upon heating (ZFH) in the unpoled and poled (1 1 0)-cut PMNT26% samples. It agrees with the phase diagram of unpoled ceramic samples at RT [5] and the phase diagram of poled crystal samples [3]. This study also found that the appearance of M phase does not depend on prior poling. The thermally induced phase transition via the M phase was observed in the unpoled and poled samples. In addition, the M phase intrinsically bridges R and C phases by means of continuous polarization rotation in the region of ~355–378 K upon heating. The difference between the unpoled and poled cases is that the M phase appears at slightly lower temperature in the unpoled sample. No [1 1 0]-polarized O domain was observed during poling along [1 1 0] at any field strength up to 45 kV/cm, and instead a single homogenous R phase was obtained. This result is very different from the (0 0 1)-cut PMNT24% crystal, which exhibits network-like [0 0 1] T domain chains while the poling was applied along [0 0 1] at 44 kV/cm [6]. No microcracking was found in the *E*-field dependent study.

Acknowledgment

The authors would like to thank Dr. Haosu Luo for the crystal. This work was supported by DoD EPSCoR Grant no. N00014-02-1-0657 and NSC Grant no. 93-2112-M-030-001.

References

[1] B. Noheda, Curr. Opin. Solid St. M. 6 (2002) 27.
[2] C.-S. Tu, V.H. Schmidt, I.-C. Shih, R. Chien, Phys. Rev. B(R) 67 (2003) 020102.
[3] C.-S. Tu, R.R. Chien, F.-T. Wang, V.H. Schmidt, P. Han, Phys. Rev. B(R) 70 (2004) 220103.
[4] V.H. Schmidt, R. Chien, I.-C. Shih, C.-S. Tu, AIP Conf. Proc. 677 (2003) 160.
[5] A.K. Singh, D. Pandey, Phys. Rev. B 67 (2003) 064102.
[6] R.R. Chien, V.H. Schmidt, C.-S. Tu, L.-W. Hung, H. Luo, Phys. Rev. B 69 (2004) 172101.